Bioresource Technology 403 (2024) 130850

Contents lists available at ScienceDirect

Bioresource Technology

journal homepage: www.elsevier.com/locate/biortech

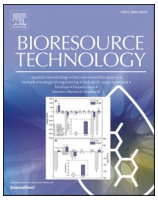

Quality of cellulose and biostimulant extracts from *Oedogonium calcareum* cultivated during primary wastewater treatment

Nethmie Jayasooriya [a,b,*], Marie Magnusson [a,b], Chanelle Gavin [c], Christian Gauss [c], Rupert Craggs [d], Christopher N. Battershill [a,b], Christopher R.K. Glasson [a,b]

[a] Coastal Marine Field Station, School of Science, University of Waikato, Tauranga, New Zealand
[b] Environmental Research Institute, The University of Waikato, Tauranga, New Zealand
[c] School of Engineering, Faculty of Science and Engineering, University of Waikato, Hamilton, New Zealand
[d] National Institute of Water and Atmospheric Research Ltd. (NIWA), Hamilton, New Zealand

GRAPHICAL ABSTRACT

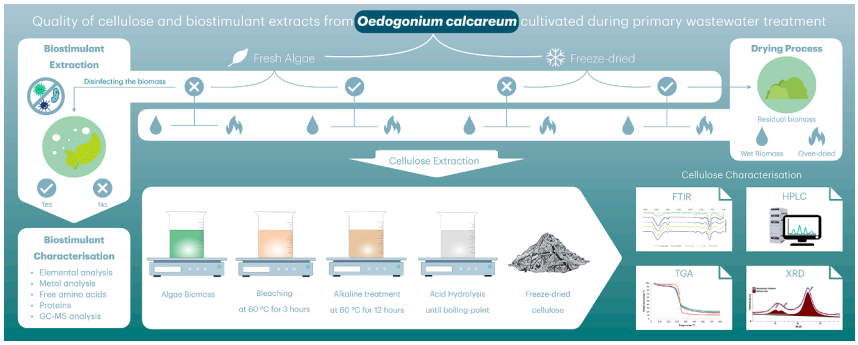

ARTICLE INFO

Keywords:
Biorefinery
Macroalgae polysaccharides
Biomass utilization
Bioremediation
Filamentous macroalgae

ABSTRACT

A practical two-product cascading biorefinery was developed to extract a biostimulant and cellulose from the freshwater filamentous macroalga *Oedogonium calcareum* grown while treating primary wastewater. Biostimulant production provides a valuable extract with production of disinfected residual biomass for further product development. Both *Escherichia coli* and F-specific RNA bacteriophage, indicators of human pathogens contamination, were absent from the residual biomass. The chemical composition of the biostimulant was complex, consisting of growth-promoting substances, free amino acids, and minerals. The *O. calcareum* cellulose fractions yielded between 9.5% and 10.1% (w/w) with purities from 84% to 90% and closely resembled microcrystalline cellulose. Biostimulant extraction improved cellulose quality by increasing crystallinity from 59% to 62%. Biomass condition, drying process, and biostimulant production influenced the crystallinity index. This study demonstrates a two-step process of biostimulant and cellulose extraction from wastewater-grown *Oedogonium*, simultaneously disinfecting biomass and isolating high-quality cellulose as a sustainable alternative to conventional extraction methods.

* Corresponding author.
E-mail address: nethmiejayasooriya@outlook.com (N. Jayasooriya).

https://doi.org/10.1016/j.biortech.2024.130850
Received 1 February 2024; Received in revised form 14 May 2024; Accepted 14 May 2024
Available online 16 May 2024

1. Introduction

Globally, 60% of nitrogen and phosphorus-rich primary treated municipal wastewater is released untreated into streams, rivers, lakes, and coastal waters increasing eutrophication in adjacent aquatic ecosystems (Neveux et al., 2018). However, the cost of the implementation and operation of advanced wastewater treatment technologies to reduce this impact is a significant impediment to upgrading many primary wastewater treatment plants (WWTPs) (Lyu et al., 2020). Microalgal pond systems are widely known to offer a low-cost alternative to treat point source nitrogen and phosphorus-rich wastewaters with the additional benefit of nutrients being assimilated into algal biomass (Sutherland et al., 2020). Recently, there has been increasing interest in cultivating freshwater filamentous macroalgae in nutrient rich wastewaters (Hariz et al., 2023) as macroalgae are typically easier to harvest than microalgae. Additionally, the algal biomass is suitable as a feedstock for product development (Neveux et al., 2020).

The filamentous macroalgal genus *Oedogonium* has been identified as a high performer for bioremediation of wastewater due to its broad ecological distribution, and high productivity (syn. with its capacity to take up nutrients) over varied environmental conditions (Lawton et al., 2021). *Oedogonium* biomass is also a valuable resource with applications in animal feeds (Vucko et al., 2017), biostimulants (Neveux et al., 2020), biochar/biosorbents (Kidgell et al., 2014), and cellulose (Piotrowski et al., 2020). However, the quality of biomass grown in primary effluent may be reduced due to contamination with pathogenic bacteria (e.g. *Campylobacter jejuni*, *Escherichia coli*, *Salmonella* spp. and *Vibrio cholera*) (Chahal et al., 2016), parasitic protozoa (*G. intestinalis* and *Cryptosporidium* spp.) (Berglund et al., 2017) and viruses (Hepatitis A, Hepatitis E, Echovirus and Human calicivirus) (Chahal et al., 2016) limiting the range of socially acceptable products. In this regard, a preliminary disinfection step would be beneficial in a biorefinery process targeting products from the biomass.

In advanced WWTPs microbial pathogens are inactivated during tertiary treatment with chemical oxidation processes and/or UV disinfection. In the context of a cascading biorefinery using primary wastewater-grown biomass it is important to determine if the biomass is adequately disinfected during the processing conditions, in this case, the high temperature and alkali conditions of biostimulant extraction. Biostimulants extracted in this way from *Oedogonium intermedium* were demonstrated to contain proteins, minerals, and phytohormones, and enhanced adventitious root development in tomatoes and mung beans (Neveux et al., 2020). The decontaminated residual algal biomass could be further exploited to produce other products such as bioethanol and cellulose. Cellulose is used widely in textiles and high-tech materials (e.g., wound dressings, aerogels, and scaffolds for tissue engineering) and is predominantly sourced from wood. Cellulose can also be sourced from grasses, bacteria, and macroalgae, and its phytochemical properties vary depending on the organism's biosynthetic machinery and environmental conditions (Zanchetta et al., 2021). Cellulose from freshwater filamentous macroalgae has unique properties compared to cellulose extracted from terrestrial plants, such as ease of extraction due to lack of lignin (Roesijadi et al., 2010), high crystallinity (Zanchetta et al., 2021), and high specific surface area (Jmel et al., 2019), providing the opportunity to engineer new materials with unique properties and applications. However, the properties of cellulose isolated from *Oedogonium* species grown in primary wastewater, and the influence of biostimulant extraction and drying processes on disinfection and product quality remains unclear.

Therefore, the objectives of this study were to develop a feasible two-product cascading biorefinery suitable for *Oedogonium* grown in primary wastewater. A biostimulant was targeted as the first product in the cascade and to determine if this process would also disinfect the biomass, while a high-quality cellulose was targeted as a second product. The chemical characteristics of the biostimulant are reported, including contents of total dissolved solids, polysaccharides, phytohormones, proteins, ash, and minerals. The effect of drying and biostimulant production on the yield and quality of cellulose isolated from *Oedogonium calcareum* was determined using a range of physico-chemical measures.

2. Materials and methods

2.1. Materials

Microcrystalline cellulose (MCC) (Product No: 435236), hydrochloric acid (Product No: 258148), sodium chlorite (Product No: 244155), sodium acetate (Product No: S2889), sodium hydroxide (Product No: S5881), sulfuric acid (Product No: 258105), 2-deoxy- d-glucose (Product No: G8270), D-(+)-glucose (Product No: D6134), D-(+)-mannose (Product No: M2069), D-(+) galacturonic acid monohydrate (Product No: PHR9231), L-(+) rhamnose (Product No: R3875), fucose (Product No: F2252), D-(+)- xylose (Product No: X3877), 1-phenyl-3-methyl-5-pyrazolone (PMP) (Product No: M70800), formic acid (Product No: 27001), ammonium solution (Product No: A/3295/pb05), ninhydrin (Product No: N4876), bovine serum albumin (BSA) (Product No: B3883), arginine (Product No: A8094), were purchased from Sigma Aldrich, chloroform (Product No: 200-663-8) was from MERCK and used as received.

2.2. Experimental design

This study aimed to assess the effect of biostimulant extraction and drying process of primary wastewater-grown *O. calcareum* biomass on disinfection, yield and quality of cellulose produced. A three-factor experimental design to quantify the effect of three treatments; treatment 1: biomass was either fresh or freeze-dried; treatment 2: biostimulant production, the biomass was extracted with 0.1 M potassium hydroxide; treatment 3: the biomass was either used wet or oven-dried at 40 °C for 48 h for cellulose extraction (Fig. 1). Note that treatments for T5 and T6 were the same, giving a total of seven discrete treatments per batch of biomass.

To assess the potential use of *Oedogonium* cellulose in materials, characterisation was conducted using Fourier Transform Infrared, X-ray Diffraction and Scanning electron microscopy, and Thermogravimetric Analysis to determine bonding, morphology and thermal stability, respectively.

2.3. Cultivation of biomass

In this study, *Oedogonium* cf. *calcareum* Cleve ex Wittrock 1870 (Lawton et al., 2021) cultures were grown in an outdoor tank under high nutrient loads (14 mg/L of N and 1.2 mg/L of P), at the Facility for Aquaculture Research of Macroalgae at the University of Waikato (UoW), Tauranga, New Zealand. *Oedogonium* samples grown on primary effluent were supplied by National Institute of Water and Atmospheric Research (NIWA), Hamilton, New Zealand to assess the efficacy of biostimulant extraction (alkaline treatment) on disinfection of faecal indicator bacteria and viruses. The ammonia and phosphate concentrations of primary effluent at the NIWA facility were measured fortnightly, and the average concentrations were 40 mg/L and 10 mg/L, respectively. Three batches of *O. calcareum* biomass were cultivated over three consecutive production cycles (2 weeks per cycle). Harvested biomass was subdivided (7 x 100 g fresh weight) and stored in polyethylene resealable bags at −20 °C prior to processing. Three samples (approximately 100.0 (±) 0.01 g) from each batch were freeze-dried (Buchi Lyovapor L-200) and milled using a domestic blender (<0.5 mm particle size), and the rest were stored frozen at −20 °C until further use. The freeze-dried samples were used to determine fresh weight to dry weight ratios (FW:DW) for each harvest of biomass. FW to DW ratios were used to standardise the total solids of biomass in treatments that used fresh biomass to those that used dried biomass.

2.4. Biostimulant production

Biostimulant was prepared using a published method (Neveux et al., 2020) with some modifications. Briefly, fresh (100 g) or equivalent mass of milled freeze-dried biomass (~20.0 g) (i.e., always corresponding to a dry weight loading of 2% w: v) was extracted with 1 L of KOH (0.1 M, pH = 13) at 70 °C for 3 h with stirring using a mechanical stirrer at a speed of 400 rpm. The residual biomass was separated from the extract by filtration using a 20 μm mesh and the alkaline liquid extract was stored at −20 °C until further use. The residual biomass was subjected to further processing according to the experimental design (Fig. 1) and cellulose production as per section 2.4.

2.5. Extraction of cellulose

Cellulose from (20.0 (±) 0.01 g freeze-dried) *O. calcareum* biomass or residual biomass was extracted following the three step method reported in (Mihranyan et al., 2004). To achieve satisfactory homogeneity, a mechanical stirrer was used at a speed of 400 rpm. Step 1: biomass was treated with 36.17 g of $NaClO_2$ in 1L of acetate buffer (0.1 M, pH = 4) at 60 °C for 3 h. Step 2: Biomass was treated with 1L of NaOH (0.5 M, pH = 13) at 60 °C for 12 h. Step 3. Biomass was treated with 1L of HCl (5% w/w, pH = 1) heated until boiling, cooled, washed until neutral pH and freeze-dried to obtain cellulose material. Between each step, successive washings of the biomass were carried out until neutral (pH = 7) by first separating the solids (centrifugation at 3214 Relative Centrifugal Force (RCF) for 10 min) followed by resuspension in reverse osmosis (RO) water and centrifugation again (at 3214 RCF for 10 min) to collect the washed solids. The weight of the freeze-dried cellulose was recorded to obtain the yield. The freeze-dried cellulose fractions were stored in sealed plastic bags at room temperature to prevent moisture absorption and degradation until further use.

2.6. Characterisation of biostimulant and cellulose products

Elemental analysis (% C, N, and S) was carried out on freeze-dried *O. calcareum* biomass, biostimulant and cellulose samples using Gas Chromatography – Thermal Conductivity Detector and ash content was determined by microashing by OEA labs (https://www.oealabs.com, Callington, UK). Total dissolved solids in biostimulants were determined gravimetrically by weighing the residual solid (mg) from freeze-dried samples of biostimulant (10 mL). Results are reported in mg/mL. Residual biomass samples were analysed for F-specific RNA (fRNA) bacteriophage and *E. coli* at the Institute of Environmental Science and Research, Christchurch. Enumeration of fRNA bacteriophage was carried out using a Single Agar Layer (SAL) technique; Method 1602 (USEPA, 2001) and *Escherichia coli* was enumerated using a pour-plate method.

2.6.1. Free amino acids and protein composition of biostimulant extract

Free amino acids (FAA) in the biostimulant extract were analysed by a modified ninhydrin protocol using arginine (2.5–40 μg/mL) as the standard (Zhu et al., 2009). Biostimulant extract was diluted (dilution factor (DF) of 100) with RO water, and the diluted sample (250 μL) was treated with ninhydrin reagent (250 μL, pH 5.5) prepared as per (Starcher, 2001). This solution was then heated at 100 °C for 10 min in a water bath to allow derivatisation. After cooling to room temperature the derivatised analyte solution (200 μL) was transferred to a polystyrene 96-well plate and the absorbance was measured at 575 nm (Starcher, 2001) using a BMG Labtech SPECTROstar Nano. FAA concentrations are reported as μg of FAA/ mL of biostimulant extract. Protein content in the biostimulant extract was analysed using (BSA) as the standard. The diluted biostimulant extracts (DF of 100 with RO water) and the BSA samples (in the range of 15–250 μg/mL) were hydrolysed in NaOH (2.1 mL, 13.5 M) in a heating block at 120 °C for 20 min (Zhu et al., 2009). After cooling the samples, hydrolysate (400 μL) was neutralized by adding glacial acetic acid (500 μL). Then, the neutralized samples (250 μL) were treated with ninhydrin reagent (250 μL) and heated in a water bath for 10 min at 100 °C and following cooling to room temperature the absorbances of samples were measured as for the FAA described above. The total protein content of biostimulant extracts is reported as μg BSA equivalents/mL of biostimulant extract.

2.6.2. Metals analysis

Metal analysis of the biostimulant extracts was performed in helium mode using an Agilent 8900 Inductively Coupled Plasma-Mass Spectrometer (ICP-MS; Agilent Technologies, Santa Clara, California, USA) controlled by MassHunter Workstation (version 4.5). Freeze-dried biostimulant (100 mg) was pre-digested in a mixture of 1 mL of HNO_3 (65%) and 0.4 mL of concentrated H_2O_2 (30%) overnight at room temperature. This mixture was then heated at 80 °C for one hour. A further 0.4 mL aliquot of H_2O_2 was then added and the mixture heating at 80 °C for 30 min. The solution was cooled and diluted to 50 mL with RO water. The diluted solution (15 mL) was then filtered using a 0.45 μm filter and analysed using the ICP-MS. Standards of trace elements were prepared using stock standard IV71-A, and the standards of main elements (Ca, Si, P, S, K, Fe) were prepared using single-element standards (Inorganic Ventures, Christiansburg, VA, USA)

2.6.3. Non-targeted gas chromatography-mass spectrometry (GC–MS) profiling of biostimulant

The freeze-dried biostimulant extracts were analysed following (Rawlinson et al., 2015) to detect phytohormones. Briefly, freeze-dried biostimulant samples and standards (10 mg) were dissolved in NaOH (200 μL, 1% w/v) in a 1.5 mL Eppendorf tube followed by addition of deuterated cinnamic acid (20 μL of 20 μg/mL in methanol), methanol (147 μL) and pyridine (34 μL). The suspension was vortexed for 30 s to ensure proper mixing. Into this suspension, 20 μL of methyl chloroformate (MCF) was added and vortexed for 30 s. The latter process was

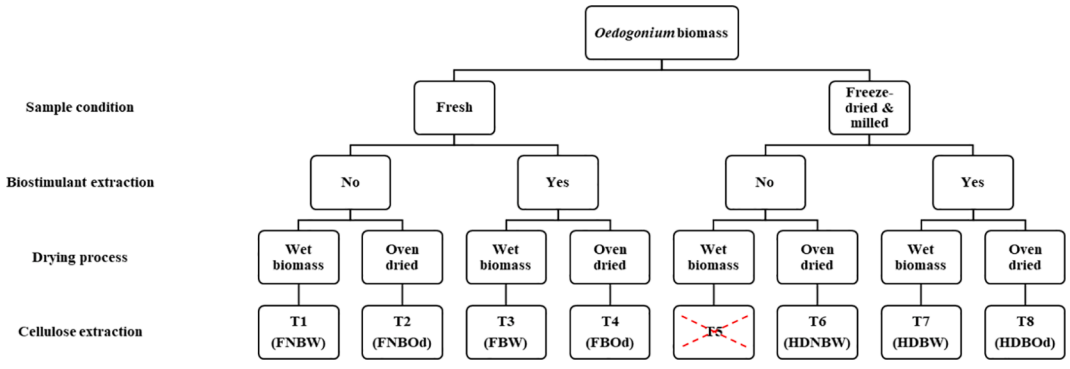

Fig. 1. Experimental Design.

repeated before the addition of chloroform (400 μL) and sodium bicarbonate solution (400 μL, 50 mM). This mixture was vortexed for 15 s prior to separation of organic and aqueous phases with centrifugation (60 sec at 16,000 g). The organic layer was transferred into a second 1.5 mL Eppendorf centrifuge tube and dried over anhydrous sodium sulfate prior to transferring 100 μL to a 2 mL Shimadzu GC–MS vial fitted with a 250 μL glass insert (CAT number: 226–50523–00). Samples were analysed on a Nexis GC-2030 − Shimadzu gas chromatograph coupled with a single quadrupole mass spectrometer (GCMS-QP2020 NX) using an SH-I-5Sil MS column (30 m x 0.25 mm x 0.25 μm). The ion source used electron ionisation (EI), and the MS was run in scan mode to identify the analytes. Helium was used as the carrier at a flow rate of 0.96 mL/min. The flow control mode was set to linear velocity, and the pressure was set to 9.0 psi. The injection volume was set to 2 μL in spitless injection mode. The oven temperature for the method was set at 80 °C, held for 1 min and ramped up to 320 °C at a rate of 10 °C /minute, and held for 2 min. Amino acids, fatty acids, and other compounds, with a similarity index exceeding 85%, were identified in the biostimulant with reference to the GC–MS solution NIST 17 library.

2.6.4. Constituent sugar analysis

Cellulose samples (10 mg) were hydrolysed in H_2SO_4 (300 μL, 13 M) at 30 °C for 30 min, prior to dilution to 0.72 M H_2SO_4 with Type 1 water and further hydrolysed at 120 °C for 40 min (Manns et al., 2014). Hydrolysates were derivatised with PMP as per the protocol by (Rozaklis et al., 2002) with some modifications. Briefly, hydrolysed cellulose (100 μL) was neutralised with NaOH (71.6 μL, 2 M) prior to the addition of PMP-derivatising reagent (400 μL), and internal standard 2-Deoxyglucose (40 μL of 1 mg/mL). The reaction mixture was then heated at 70 °C for 90 min with stirring. On completion the samples were neutralized with formic acid (400 μL, 0.8 M), and the excess PMP extracted with $CHCl_3$ (750 μL) prior to centrifugation (5 min at 13,000 g) of the aqueous phase. The aqueous supernatant was transferred to a HPLC vial and analysed with a Shimadzu LC-20AD Prominence fitted with a Restek Raptor C18 column (5 μm particle size, 150 mm x 4.6 mm) with an oven temperature of 30 °C and flow rate of 0.8 mL/min. Samples (5 μL) were injected and fractionated using a gradient elution (25% B 0–15 min, 25–100% B at 15–40 min, 100% B 40–55 min, 25% B 55–60 min) at pH 7 using 0.1 M phosphate buffer in 10% acetonitrile (v/v) (solvent A) and 0.1 M phosphate buffer in 17% acetonitrile (v/v) (solvent B). Peak areas were obtained using Shimadzu LabSolutions software. Monosaccharides (fucose, arabinose, rhamnose, galactose, glucose, xylose, mannose, galacturonic acid, glucuronic acid, and iduronic acid) were quantified using response calibration curves of standards with concentrations ranging between 0.05 – 3 mg/mL. The results were reported as w/w% of the anhydrous sugar content.

2.6.5. Attenuated total reflectance-Fourier transform infrared spectroscopy (ATR-FTIR)

FTIR spectra (4000 – 400 cm^{-1}) of dried *O. calcareum* and extracted cellulose fractions were recorded at room temperature using a Shimadzu IRSpirit fitted with a QATR-S accessory with an average number of 45 scans per sample. Microcrystalline cellulose (MCC) was used as the reference. The data were ATR and baseline corrected and normalized relative to 1022 cm^{-1} peak using Shimadzu LabSolutions IR software.

2.6.6. Scanning electron microscopy (SEM)

The morphology of extracted cellulose was visualised by scanning electron microscopy with a Hitachi Regulus SU8230 FE-SEM. To prepare the freeze-dried cellulose samples for SEM, they were attached to the sample disks using double-sided carbon tape and sputter-coated with fine platinum particles with a Q150V Plus sputter coater.

2.6.7. Thermogravimetric analysis (TGA)

The thermal stability of extracted cellulose and MCC was determined using a Netzsch Jupiter STA449 F5 instrument. Samples (10 mg) were analysed in alumina crucibles using a temperature program ranging between 30–800 °C with a constant heating rate of 10 °C/min and an argon flow rate of 50 mL/min. The ash content was calculated as the weight remaining at the end of the heating program.

2.6.8. X-ray diffraction

The crystallinity of extracts of cellulose from *O. calcareum* biomass and MCC was determined using a Panalytical Empyrean XRD using CuKα (λ = 1.54 nm) radiation equipped with a PixCel linear detector. Data was collected over a scan range of 10° − 40° at a step of 0.01° and an equivalent exposure time of 40 s with a voltage and current of 45 kV and 40 mA, respectively. The crystallinity index (CI) of cellulose was calculated according to Equation (1) (Segal et al., 1959) where I_{110} (crystalline peak of cellulose Iα) refers to the intensity of the peak at 2θ ~ 22°, and I_{am} (amorphous region of cellulose) refers to the intensity at 2θ = 18.5°.

$$Crystalinityindex(\%) = \frac{I_{110} - I_{am}}{I_{110}} \times 100 \quad (1)$$

The algal cellulose data was fitted to a simulated pattern of cellulose Iα (the dominant cellulose polymorph in most macroalgae (Moon et al., 2011; Onyianta et al., 2020)) using HighScore® Plus software. The crystal information file for cellulose Iα was obtained from (Nishiyama et al., 2003). Commercially sourced MCC was analysed under the same conditions as a reference.

2.6.9. Statistical analysis

In this study, all experiments were carried out in triplicate using biomass cultivated in three different production cycles (each harvest was 2 weeks apart). Data was analysed using non-parametric permutational multivariate analysis of variance (PERMANOVA) in PRIMER7 software using Euclidian distance resemblance matrices, TYPE III (partial) sum of squares and based on 9,999 unrestricted permutations of raw data (Clarke & Gorley, 2015). One-way PERMANOVA was used to test the effect of the biomass condition (fresh or freeze-dried) on the C, N, ash, FAA and protein contents in the biostimulant. To compare the overall effect on the quality of cellulose in terms of purity, yield, chemical composition, and crystallinity index, three-way PERMANOVAs were run with “biomass condition” (fresh or freeze-dried), “biostimulants extraction” (yes or no), and “drying process” (oven dried or wet) as fixed factors. Permutation t-tests were conducted to examine pairwise differences between factors (see supplementary material). The measure of effect size (η^2) between factors was calculated using the following equation (Eq. (2)), where: SS_{factor} refers to the sum of squares of a particular factor and SS_{total} refers to the total sum of squares.

$$\eta 2(\%) = \frac{SS_{factor}}{SS_{total}} \times 100 \quad (2)$$

3. Results and discussion

This study demonstrated the suitability of a cascading biorefinery process to sequentially extract a biostimulant and a high-quality cellulose product from *O. calcareum* biomass cultivated in primary wastewater. The biostimulant was rich in amino acids, fatty acids and minerals, and the extraction process disinfected the residual biomass improving the quality of cellulose obtained.

3.1. Biostimulant characterisation

One of the primary goals of this study was to determine if biostimulant extraction effectively disinfected the remaining wastewater-grown algal biomass. Microbiological assessment of the remaining algal biomass showed that biostimulant extraction was an effective disinfection step, resulting in levels of fRNA (0 Plaque forming units (PFU)/100 mL) bacteriophage and *E.Coli* (no *E.coli* present) that were

below levels of detection. The use of high pH conditions, specifically above pH 12, combined with heat treatments (above 65 °C), has been proven to denature the intact RNA of microbial pathogens below the limit of detection (Lemire et al., 2016). Therefore, this confirms the biostimulant extraction process carried out in 0.1 M KOH (pH = 13), is an effective method for disinfecting the biomass, ensuring its safety for further applications.

Full compositional analysis of the biostimulant samples extracted from fresh or freeze-dried biomass are detailed in. Briefly, freeze drying the biomass had no effect on the C, N, ash, and protein content, but did increase the free amino acid content ($p = 0.0496$) (30% lower in the biostimulant produced from fresh than from freeze-dried biomass). While the recovery of N from the biomass into biostimulant was 16.5%, the nitrogen content (13,800 ppm) of the biostimulants was 9-fold higher than the biostimulant reported by Neveux *et al* (1,500 ppm) (Neveux et al., 2020), reflecting the exceptionally high nitrogen content of the biomass used here (8.2 – 9.4% of dw biomass). Potassium made up approximately 93% of the elements detected through ICP-MS, and along with P, S, Ca, Na, Ca, Mg, and Fe made up over 99% of the metals, and this was similar to (Neveux et al., 2020). The high content of ash is a result of the production process (63% of the total ash resulted from the KOH solution), and while active organic compounds contribute most of the plant growth promoting effects in an algal biostimulant, this inorganic potassium helps regulate the water status of plants, controls photosynthesis through the opening and closing of stomata, and influences meristematic growth (Hernández-Herrera et al., 2014). With the method used here, only phenyl acetic acid, a known auxin with growth-promoting activity (Cook, 2019), was detected. Neveux *et al.* reported an auxin-like activity equivalent to 5×10^{-5} M indole-3-butyric acid and the presence of all five major classes of phytohormones (abscisic acid and metabolites, cytokinins, auxins, gibberellins, and ethylene) in their alkali extract of *O. intermedium*. Differences in composition between the biostimulants produced here and in Neveux et al. (2020), are expected, with the current study using a lower biomass loading (2% w/v vs. 5% w/v) and harsher extraction conditions (0.1 M KOH vs. 0.01 M KOH), which were chosen specifically to ensure disinfection of the biomass feedstock. In addition to *Oedogonium*, freshwater macroalgae species such as *Cladophora* and *Rhizoclonium* have been identified for their potential in wastewater bioremediation (Zrimec et al., 2022; Hariz et al., 2023). Previous research indicates that *Cladophora* species contain high levels of proteins (16% to 21.5% of dry weight), fatty acids comprising 11.7% of dry weight, micro and macro-elements, vitamins and phytohormones, all of which stimulate plant growth (Nutautaitė et al., 2021; Lewandowska et al., 2022). Specifically, *Cladophora glomerata* biostimulant extracts, obtained through ultrasound extraction in distilled water, have demonstrated significant effects on the growth parameters of soybean and red radish, such as increased yield, root length, and plant height, compared to control conditions (Dziergowska et al., 2021; Lewandowska et al., 2022). Mungmai et al. (2014) reported presence of proteins (0.3–0.4 ng/g of crude weight) and a series of amino acids in *Rhizoclonium hieroglyphicum* such as phenylalanine, alanine, proline and serine (Mungmai et al., 2014). Nevertheless, a range of amino acids and fatty acids (see supplementary material) demonstrated to be important for plant health and nutrition (Yang et al., 2020) were identified in this study. Furthermore, Stirk et al. have mentioned that storing the biomass at −20 °C in the dark can preserve the biostimulant properties such as proteins, lipid and fatty acid content the up to fifteen months without a significant decrease (Stirk et al., 2021). This suggests that similar long-term storage conditions could be applicable for the biostimulant produced in this study. Additionally, in line with the regulatory framework, this biostimulant extract would need to comply with the European Union Fertilising Products Regulation (EU) 2019/1009, which recognises products that enhance plant nutrition processes, to fit the macroalgae-derived biostimulant into the established parameters for agricultural application (Kapoore et al., 2021)

3.2. Cellulose characterisation

Cellulose was extracted from the residual (following biostimulant production) biomass or untreated *O. calcareum* biomass using a mild extraction technique that has previously been shown to yield a high purity product (Mihranyan et al., 2004). The average percentage yield of cellulose was 9.8 ± 0.3% of the dry weight biomass, ranging from 9.5 −10.1% between treatments which were not statistically different. This is lower than the cellulose contents in an *Oedogonium sp.* (24–58%) grown in municipal wastewater effluent with carbon dioxide supplementation in Minnesota, USA (Piotrowski et al., 2020). However, no quantification of purity and composition (e.g., FTIR, sugar analysis, nitrogen, or ash content), or functional analyses, were performed in that study except for the morphological analysis by SEM, and SEM micrographs of extracted cellulose in that study closely resembles the raw biomass in this study. Higher yields of cellulose have also been reported for other freshwater macroalgae species, e.g., *Cladophora glomerata* (21.6%) (Xiang et al., 2016). While the contents of cellulose clearly vary between species, growing conditions (seasonal changes/temperature, and CO_2 availability) (Piotrowski et al., 2020) and the maturity of algae (Wahlström et al., 2020) are also important drivers of cellulose content. There were significant differences in the content of C, H, and N in the cellulose between treatments due to the starting condition of the biomass (i.e., fresh vs. freeze-dried), where the starting condition of the biomass accounted for 25.6%, 26.9%, and 31.4% of the variation of C, H, and N contents of the cellulose fractions, respectively. Cellulose products had a low content of nitrogen (<1%) and ash (<1%) (Table 1), indicating that the pulping and purification processes effectively removed proteins and other biomolecules from the biomass, as well as the salts generated during the pulping process. Consistent with these indicators of purity, the cellulose samples had a high glucose content (85–90%) and a low mannose content (<0.5%), while other sugars characteristic of hemicellulose, such as xylose, rhamnose, fucose and galactose (Ren & Sun, 2010), were not detected. There was no significant difference in the glucose content of the celluloses between the treatments (see supplementary material).

3.2.1. Fourier Transform Infrared (FTIR) analysis

Cellulose has a unique FTIR fingerprint region in the range of 1800–600 cm^{-1}. To assess the quality of cellulose produced in the current study the FTIR of isolated cellulose fractions were compared with a commercial sample of MCC. All cellulose fractions from *O. calcareum* had absorbances characteristic of cellulose and were highly analogous with the spectrum obtained for MCC (see supplementary material). All spectra exhibited absorbance peaks in the 3000 to 3500 cm^{-1} region, indicating stretching and bending vibrations due to hydroxyl groups, while the peak at 2896 cm^{-1} was identified as the C-H stretching of methylene groups (Paniz et al., 2020). The O-H bending at 1654 cm^{-1} indicated the presence of absorbed water (Oh et al., 2005). Other peaks characteristic of cellulose included C-H scissoring at 1424 cm^{-1}, C-H bending at 1363 cm^{-1}, O-H in-plane bending at 1333 cm^{-1}, CH_2 wagging at 1310 cm^{-1}, and C-O-C antisymmetric ring stretching at 1158 cm^{-1}. Furthermore, 1054 cm^{-1} and 1029 cm^{-1} peaks were associated with C-O stretching and C-O deformation at C6, respectively (Paniz et al., 2020). The peak at 898 cm^{-1} is attributed to the C-O-C asymmetric stretch of β-glycosidic linkages (Wahlström et al., 2020).

In addition, the broad band emerging at 2850 cm^{-1} in the untreated algae biomass is attributed to aliphatic chains (e.g., lipids) in algae biomass (Paniz et al., 2020). The absence of the peak at 2850 cm^{-1} in T6-T8 samples indicate successful removal of lipids in algae. Although this peak is not as distinct as in the raw biomass, this peak is still evident in other cellulose samples (T1-T4), indicating incomplete lipid removal during the pre-treatment process.

3.2.2. X-ray diffraction

The crystal structure and crystallinity index of cellulose samples

Table 1
Yield and quality of cellulose products from each treatment (T) expressed *O. calcareum* biomass. Yield is expressed as % dry weight biomass (% dw) and quality measures (C, H, N, ash, glucose (Glu) and mannose (Man) as % w/w of cellulose product. Entries are expressed as averages ± standard deviations (n = 3). *(Treatment abbreviations are as follows F = Fresh, HD = freeze-dried biomass, NB = no biostimulant extraction, B = biostimulant extraction W = wet biomass, Od = oven-dried biomass after biostimulant extraction)*.

Treatment	Yield	C	H	N	Ash	Glu	Man
	(% dw)	(% w/w)					
T1 (FNBW)	10.0 ± 0.1	45.5 ± 1.2	7.0 ± 0.2	0.40 ± 0.2	0.1 ± 0.1	89.6 ± 0.1	0.4 ± 0.1
T2 (FNBOd)	10.0 ± 0.2	45.0 ± 0.7	6.9 ± 0.1	0.2 ± 0.1	0.1 ± 0.1	85.0 ± 5.2	0.3 ± 0.1
T3 (FBW)	9.5 ± 0.2	44.0 ± 1.2	6.7 ± 0.2	0.2 ± 0.2	<0.1 ± 0.1	87.6 ± 4.5	0.4 ± 0.1
T4 (FBOd)	9.7 ± 0.1	44.8 ± 0.4	6.8 ± 0.1	0.3 ± 0.2	0.1 ± 0.1	87.7 ± 3.6	0.5 ± 0.1
T6 (HDNBW)	9.6 ± 0.1	44.0 ± 1.4	6.7 ± 0.2	0.2 ± 0.1	<0.1 ± 0.1	90.1 ± 1.1	0.4 ± 0.1
T7 (HDBW)	9.5 ± 0.3	43.8 ± 1.3	6.6 ± 0.2	0.2 ± 0.2	0.2 ± 0.1	89.1 ± 3.1	0.4 ± 0.1
T8 (HDBOd)	9.9 ± 0.1	43.2 ± 0.3	6.6 ± 0.1	0.1 ± 0.1	0.1 ± 0.1	89.5 ± 1.1	0.4 ± 0.1

All experiments were carried out in triplicate using biomass cultivated in three different production cycles (each harvest was 2 weeks apart).

were determined by XRD and compared to MCC. Fig. 2a shows diffractograms of cellulose from different treatments of *O. calcareum* overlaid with the diffractogram of MCC. Cellulose is classified as crystalline when its crystallinity index (CI) falls within the range of 40–95%; while cellulose with CI values below this range are classified as amorphous (Quiroz-Castañeda & Folch-Mallol, 2013). The crystallinity index of *O. calcareum* (58–65%) was indicative of a moderately high crystallinity index (CI of MCC = 76.2%). These results were higher than the extracted cellulose from *Ulva lactuca* (Wahlström et al., 2020) with a crystallinity index of 48%, but lower than cellulose extracted from *Cladophora rupestris* following the method by Siddhanta et al. (Siddhanta et al., 2009) with a crystallinity index of 93.3%. The proportion of amorphous regions within the *Oedogonium* cellulose may offer an advantage by increasing susceptibility to enzymatic degradation (Ioelovich, 2021), potentially enhancing biodegradability and bioconversion processes.

In the current study, there was a significant main effect of biostimulant extraction (p = 0.0052) and a significant interaction effect between biomass condition (i.e., fresh or freeze-dried and milled) and drying process (i.e., oven dried or wet) (p = 0.0151) affecting the crystallinity index with biostimulant extraction explaining 18.2% of the variance and the interaction 12.5%. Note that T1 (FNBW) and T2 (FNBOd) cellulose samples without the disinfection step show a split in the peak at 2θ = 21.6° (Fig. 2b), possibly due to the presence of silica from diatoms present during cultivation (Flores-Rojas et al., 2021). This shows that the additional step to extract the biostimulant improved the quality of the cellulose produced.

Similar to most other cellulose sources, cellulose from macroalgae consists of cellulose I, containing the polymorphs I_α, with a triclinic crystal structure, and I_β, with a monoclinic crystal structure, typically with a higher proportion of cellulose I_α (Siddhanta et al., 2009; Moon et al., 2011; Siddhanta et al., 2013). Crystallographic data from a previous study was used to model these results with cellulose I_α structure demonstrating the characteristic peaks at 2θ = 16° and 22° and 34°, corresponding to crystal planes of cellulose I_α, (1 0 0)/(0 1 0) and (1 1 0), respectively (Nishiyama et al., 2003; French, 2014) (Fig. 2 c). While it is

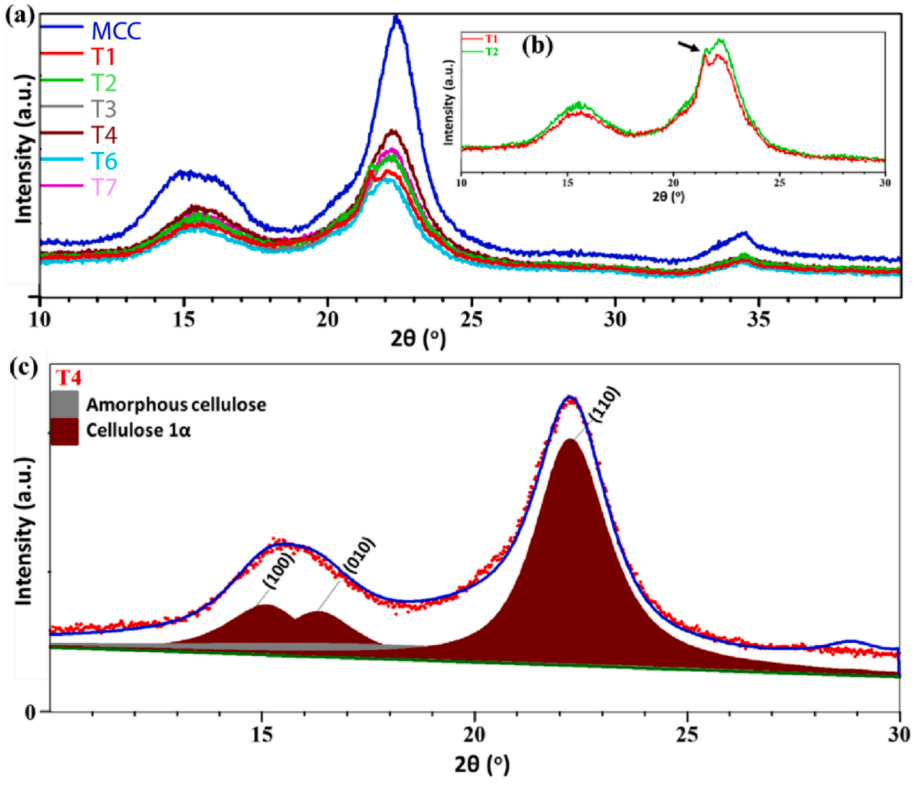

Fig. 2. X-ray diffraction pattern of (a) cellulose samples and MCC. The insert in (b) shows the shoulder peaks of T1 (FNBW) and T2 (FNBOd). (c) Experimental diffraction pattern (red dots) of T4 (FBOd) sample fitted with simulated cellulose 1α structure (blue line).

possible to observe a good fit between the experimental pattern (red dots, Fig. 2c) and the modelled profile (blue line, Fig. 2c), cellulose I_{β} may also be present in cellulose samples extracted from *O. calcareum*.

3.2.3. Thermal analysis

The raw biomass, extracted cellulose fractions, and MCC were analysed by TGA (Fig. 3). The TGA analysis indicated three distinct thermal processes. Primarily, between 50–150 °C there is a weight loss of 5–7% due to vaporisation of bound water in the *Oedogonium* cellulose samples. In a previous study, the weight loss due to bound and non-freezing water was shown to be negatively correlated with the crystallinity index (Nakamura et al., 1981). The results agree with this, as MCC with a high crystallinity index has a lower content of absorbed water (3%), and *O. calcareum* cellulose fractions with a lower crystallinity index have higher contents of water. Secondly, a weight loss of 46–55% w/w was recorded between 250–340 °C due to the thermal degradation of cellulose. Finally, a gradual decline in weight 14–19% is recorded between 350–600 °C. The most significant mass loss was initiated around 260 °C, showing that *Oedogonium* cellulose is thermally stable up to 260 °C. This thermal stability falls towards the lower end found for freshwater macroalgae and seaweeds (260–365.7 °C) (Sucaldito & Camacho, 2017; Wahlström et al., 2020; Zanchetta et al., 2021). Cellulose extracted from the seaweed *Ulva lactuca* collected along the Swedish west coast showed a thermal stability up to 260 °C (CI = 63%) (Wahlström et al., 2020). However, macroalgal cellulose extracted from the freshwater alga *Cladophora rupestris* grown in a volcanic lake in Philippines had a very high thermal stability of 365.7 ± 2.2 °C (CI = 93%) (Sucaldito & Camacho, 2017). The thermal stability has been demonstrated to be proportional to the crystallinity index of cellulose (Wahlström et al., 2020). Therefore, the low thermal stability of the cellulose from *O. calcareum* is in accordance with the measured crystallinity index (65%).

3.2.4. Morphologic characterisation

The morphology of untreated *O. calcecarum* biomass and cellulose extracts was assessed using SEM (see supplementary material). Filaments and cell structures of untreated freeze-dried *O. calcecarum* are visible, while in the extracted cellulose fractions, the cell structures are not visible demonstrating that the pulping process is effective in degrading these cell structures. Nanofibril formation requires close packing of molecules which is indicative of purified linear polysaccharides like cellulose (Wahlström et al., 2020). These intertwining fibres form sponge-like aggregate structures with pores on the surface that are likely due to water evaporation during the freeze-drying process.

Based on the findings, this two-step process can be seamlessly integrated into the existing small-scale WWTPs; implementing biomass disinfecting methods such as UV oxidation can be impractical due to high implementation and operational costs (Lyu et al., 2020). Therefore, hot alkaline extraction method used in this study may offer a practical approach, disinfecting the biomass directly at the wastewater treatment facility and ensuring safe handling for further use. Furthermore, the biostimulant drying step after biostimulant extraction did not affect the quality of cellulose, which could facilitate dry biomass transport and enhance logistical efficiency. This integration could enhance the value chain of macroalgal wastewater treatment plants and contribute to the circular economy by enabling the recovery of valuable bioproducts from wastewater-grown macroalgae feedstocks. Considering the moderately high crystallinity index, high purity and low ash content, and thermal stability up to 260 °C, *O. calcareum* cellulose has promising characteristics for potential use as a biodegradable filler in thermoplastic-based composite materials. In addition, derivatives obtained from *O. calcareum* cellulose, such as microcrystalline cellulose, cellulose nanocrystals and cellulose nanofibres, could also be used for the production of cellulose-based foams and packaging with good barrier properties (Zanchetta et al., 2021). Moreover, future work should focus on pilot-scale studies to evaluate the operational feasibility and scalability of incorporating this biorefinery process into established small-scale WWTPs.

4. Conclusion

This two-step cascading biorefinery model provides a proof-of-concept to produce disinfected and high-quality bioproducts from wastewater-grown algal biomass. Primarily, this work demonstrated that the extraction of a biostimulant also provides an effective disinfection step for macroalgae grown on primary wastewater. For the first time, the composition and structural characteristics of cellulose from *Oedogonium* were analysed. The cellulose produced had a moderately high crystallinity index and was predominantly cellulose I_{α}. Producing biostimulant and semi-crystalline *Oedogonium* cellulose improves the safe handling of biomass, and provides an alternative source of cellulose, which may be less intensive to extract compared with conventional sources.

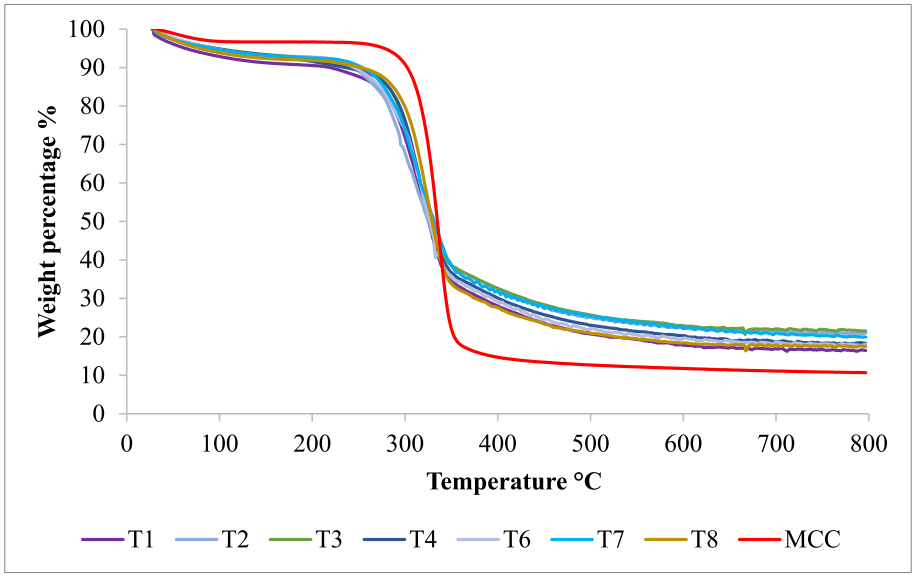

Fig. 3. Thermogravimetric analysis curves of MCC and the representative average of each harvest.

CRediT authorship contribution statement

Nethmie Jayasooriya: Writing – review & editing, Writing – original draft, Visualization, Software, Investigation, Formal analysis, Data curation. **Marie Magnusson:** Writing – review & editing, Supervision, Conceptualization. **Chanelle Gavin:** Writing – review & editing, Supervision. **Christian Gauss:** Writing – review & editing, Supervision, Formal analysis. **Rupert Craggs:** Writing – review & editing, Supervision, Funding acquisition. **Christopher N. Battershill:** Writing – review & editing, Supervision. **Christopher R.K. Glasson:** Writing – review & editing, Supervision, Conceptualization.

Declaration of competing interest

The authors declare that they have no known competing financial interests or personal relationships that could have appeared to influence the work reported in this paper.

Data availability

Data will be made available on request.

Acknowledgements

This research was funded by the New Zealand National Institute of Water and Atmospheric Research through a Ministry of Business, Innovation and Employment endeavour research programme contract number C01X1912. The authors would like to thank Dr Ari Brandenburg, Peter Randrup, Helen Turner, and Dr Stella Raynova for their technical assistance.

Appendix A. Supplementary data

Supplementary data to this article can be found online at https://doi.org/10.1016/j.biortech.2024.130850.

References

Berglund, B., Dienus, O., Sokolova, E., Berglind, E., Matussek, A., Pettersson, T., Lindgren, P.-E., 2017. Occurrence and removal efficiency of parasitic protozoa in Swedish wastewater treatment plants. Sci. Total Environ. 598, 821–827.

Chahal, C., van den Akker, B., Young, F., Franco, C., Blackbeard, J., Monis, P., 2016. Chapter Two - Pathogen and Particle Associations in Wastewater: Significance and Implications for Treatment and Disinfection Processes. In: Sariaslani, S., Michael Gadd, G. (Eds.), Advances in Applied Microbiology. Academic Press, pp. 63–119.

Clarke, K., Gorley, R., 2015. Getting started with PRIMER v7. Plymouth, Plymouth Marine Laboratory, PRIMER-E, p. 20.

Cook, S.D., 2019. An historical review of phenylacetic acid. Plant Cell Physiol. 60 (2), 243–254.

Dziergowska, K., Wełna, M., Szymczycha-Madeja, A., Chęcmanowski, J., Michalak, I., 2021. Valorization of Cladophora glomerata biomass and obtained bioproducts into biostimulants of plant growth and as sorbents (biosorbents) of metal ions. Molecules 26 (22), 6917.

Flores-Rojas, E., Schnabel, D., Justo-Cabrera, E., Solorza-Feria, O., Poggi-Varaldo, H.M., Breton-Deval, L., 2021. Using nano zero-valent iron supported on diatomite to remove acid blue dye: synthesis, characterization, and toxicology test. Sustainability 13 (24), 13899.

French, A.D., 2014. Idealized powder diffraction patterns for cellulose polymorphs. Cellul. 21 (2), 885–896.

Hariz, H.B., Lawton, R.J., Craggs, R.J., 2023. Novel assay for attached Filamentous algae productivity and nutrient removal. J. Appl. Phycol. 35 (1), 251–264.

Hernández-Herrera, R.M., Santacruz-Ruvalcaba, F., Ruiz-López, M.A., Norrie, J., Hernández-Carmona, G., 2014. Effect of liquid seaweed extracts on growth of tomato seedlings (Solanum lycopersicum L.). J. Appl. Phycol. 26, 619–628.

Ioelovich, M., 2021. Preparation, characterization and application of amorphized cellulose—A review. Polymers 13 (24), 4313.

Jmel, M.A., Anders, N., Ben Messaoud, G., Marzouki, M.N., Spiess, A., Smaali, I., 2019. The stranded macroalga Ulva lactuca as a new alternative source of cellulose: Extraction, physicochemical and rheological characterization. J. Clean. Prod. 234, 1421–1427.

Kapoore, R.V., Wood, E.E., Llewellyn, C.A., 2021. Algae biostimulants: A critical look at microalgal biostimulants for sustainable agricultural practices. Biotechnol. Adv. 49, 107754.

Kidgell, J.T., de Nys, R., Hu, Y., Paul, N.A., Roberts, D.A., 2014. Bioremediation of a complex industrial effluent by biosorbents derived from freshwater macroalgae. PLoS One 9 (2), e94706–e.

Lawton, R.J., Glasson, C.R.K., Novis, P.M., Sutherland, J.E., Magnusson, M.E., 2021. Productivity and municipal wastewater nutrient bioremediation performance of new filamentous green macroalgal cultivars. J. Appl. Phycol. 33 (6), 4137–4148.

Lemire, K.A., Rodriguez, Y.Y., McIntosh, M.T., 2016. Alkaline hydrolysis to remove potentially infectious viral RNA contaminants from DNA. Virol. J. 13 (1), 88.

Lewandowska, S., Marczewski, K., Kozak, M., Ohkama-Ohtsu, N., Łabowska, M., Detyna, J., Michalak, I., 2022. Impact of freshwater macroalga (Cladophora glomerata) extract on the yield and morphological responses of Glycine max (L.) Merr. Agriculture 12 (5), 685.

Lyu, Y., Ye, H., Zhao, Z., Tian, J., Chen, L., 2020. Exploring the cost of wastewater treatment in a chemical industrial Park: Model development and application. Resour. Conserv. Recycl. 155, 104663.

Manns, D., Deutschle, A.L., Saake, B., Meyer, A.S., 2014. Methodology for quantitative determination of the carbohydrate composition of brown seaweeds (Laminariaceae). RSC Adv. 4 (49), 25736–25746.

Mihranyan, A., Andersson, S.-B., Ek, R., 2004. Sorption of nicotine to cellulose powders. Eur. J. Pharm. Sci. 22 (4), 279–286.

Moon, R.J., Martini, A., Nairn, J., Simonsen, J., Youngblood, J., 2011. Cellulose nanomaterials review: structure, properties and nanocomposites. Chem. Soc. Rev. 40 (7), 3941–3994.

Mungmai, L., Jiranusornkul, S., Peerapornpisal, Y., Sirithunyalug, B., Leelapornpisid, P., 2014. Extraction, characterization and biological activities of extracts from freshwater macroalga [Rhizoclonium hieroglyphicum (C. Agardh) Kützing] cultivated in Northern Thailand. Chiang. Mai J. Sci. 41, 14–26.

Nakamura, K., Hatakeyama, T., Hatakeyama, H., 1981. Studies on bound water of cellulose by differential scanning calorimetry. Text. Res. J. 51 (9), 607–613.

Neveux, N., Bolton, J.J., Bruhn, A., Roberts, D.A., & Ras, M. (2018). The Bioremediation Potential of Seaweeds: Recycling Nitrogen, Phosphorus, and Other Waste Products. In *Blue Biotechnology* (pp. 217-239).

Neveux, N., Nugroho, A.A., Roberts, D.A., Vucko, M.J., de Nys, R., 2020. Selecting extraction conditions for the production of liquid biostimulants from the freshwater macroalga Oedogonium intermedium. J. Appl. Phycol. 32 (1), 539–551.

Nishiyama, Y., Sugiyama, J., Chanzy, H., Langan, P., 2003. Crystal structure and hydrogen bonding system in cellulose Iα from synchrotron X-ray and neutron fiber diffraction. J. Am. Chem. Soc. 125 (47), 14300–14306.

Nutautaitė, M., Vilienė, V., Racevičiūtė-Stupelienė, A., Bliznikas, S., Karosienė, J., Koreivienė, J., 2021. Freshwater Cladophora glomerata biomass as promising protein and other essential nutrients source for high quality and more sustainable feed production. Agriculture 11 (7), 582.

Oh, S.Y., Yoo, D.I., Shin, Y., Seo, G., 2005. FTIR analysis of cellulose treated with sodium hydroxide and carbon dioxide. Carbohydr. Res. 340 (3), 417–428.

Onyianta, A.J., O'Rourke, D., Sun, D., Popescu, C.-M., Dorris, M., 2020. High aspect ratio cellulose nanofibrils from macroalgae Laminaria hyperborea cellulose extract via a zero-waste low energy process. Cellul. 27 (14), 7997–8010.

Paniz, O.G., Pereira, C.M.P., Pacheco, B.S., Wolke, S.I., Maron, G.K., Mansilla, A., Colepicolo, P., Orlandi, M.O., Osorio, A.G., Carreño, N.L.V., 2020. Cellulosic material obtained from Antarctic algae biomass. Cellul. 27 (1), 113–126.

Piotrowski, M.J., Graham, L.E., Graham, J.M., 2020. Temperate-zone cultivation of Oedogonium in municipal wastewater effluent to produce cellulose and oxygen. J. Ind. Microbiol. Biotechnol. 47 (2), 251–262.

Quiroz-Castañeda, R.E., Folch-Mallol, J.L., 2013. Hydrolysis of biomass mediated by cellulases for the production of sugars. *Sustainable degradation of lignocellulosic biomass techniques, applications and commercialization*. INTECH 119–155.

Rawlinson, C., Kamphuis, L.G., Gummer, J.P.A., Singh, K.B., Trengove, R.D., 2015. A rapid method for profiling of volatile and semi-volatile phytohormones using methyl chloroformate derivatisation and GC–MS. Metabolomics 11 (6), 1922–1933.

Ren, J.-L., Sun, R.-C., 2010. Hemicelluloses. Cereal Straw as a Resource for Sustainable Biomaterials and Biofuels 1, 73–130.

Roesijadi, G., Jones, S.B., Snowden-Swan, L.J., Zhu, Y. (2010). *Macroalgae as a biomass feedstock: a preliminary analysis.* Pacific Northwest National Lab.(PNNL), Richland, WA (United States).

Rozaklis, T., Ramsay, S., Whitfield, P., Ranieri, E., Hopwood, J., Meikle, P., 2002. Determination of Oligosaccharides in Pompe Disease by Electrospray Ionization Tandem Mass Spectrometry. Clin. Chem. 48, 131–139.

Segal, L., Creely, J.J., Martin Jr, A., Conrad, C., 1959. An empirical method for estimating the degree of crystallinity of native cellulose using the X-ray diffractometer. Text. Res. J. 29 (10), 786–794.

Siddhanta, A.K., Prasad, K., Meena, R., Prasad, G., Mehta, G.K., Chhatbar, M.U., Oza, M. D., Kumar, S., Sanandiya, N.D., 2009. Profiling of cellulose content in Indian seaweed species. Bioresour. Technol. 100 (24), 6669–6673.

Siddhanta, A.K., Kumar, S., Mehta, G.K., Chhatbar, M.U., Oza, M.D., Sanandiya, N.D., Chejara, D.R., Godiya, C.B., Kondaveeti, S., 2013. Cellulose Contents of Some Abundant Indian Seaweed Species. Nat. Prod. Commun. 8 (4), 1934578X1300800423.

Starcher, B., 2001. A ninhydrin-based assay to quantitate the total protein content of tissue samples. Anal. Biochem. 292 (1), 125–129.

Stirk, W.A., Bálint, P., Vambe, M., Kulkarni, M.G., van Staden, J., Ördög, V., 2021. Effect of storage on plant biostimulant and bioactive properties of freeze-dried Chlorella vulgaris biomass. J. Appl. Phycol. 33 (6), 3797–3806.

Sucaldito, M.R., Camacho, D.H., 2017. Characteristics of unique HBr-hydrolyzed cellulose nanocrystals from freshwater green algae (Cladophora rupestris) and its reinforcement in starch-based film. Carbohydr. Polym. 169, 315–323.

Sutherland, D.L., Park, J., Heubeck, S., Ralph, P.J., Craggs, R.J., 2020. Size matters – Microalgae production and nutrient removal in wastewater treatment high rate algal ponds of three different sizes. Algal Res. 45, 101734.

USEPA. (2001). *Male-specific (F+) and somatic coliphage in water by single agar layer (SAL) procedure.* U.S. Environmental Protection Agency Report 38p.

Vucko, M.J., Cole, A.J., Moorhead, J.A., Pit, J., de Nys, R., 2017. The freshwater macroalga Oedogonium intermedium can meet the nutritional requirements of the herbivorous fish Ancistrus cirrhosus. Algal Res. 27, 21–31.

Wahlström, N., Edlund, U., Pavia, H., Toth, G., Jaworski, A., Pell, A.J., Choong, F.X., Shirani, H., Nilsson, K.P.R., Richter-Dahlfors, A., 2020. Cellulose from the green macroalgae Ulva lactuca: isolation, characterization, optotracing, and production of cellulose nanofibrils. Cellul. 27 (7), 3707–3725.

Xiang, Z., Gao, W., Chen, L., Lan, W., Zhu, J.Y., Runge, T., 2016. A comparison of cellulose nanofibrils produced from Cladophora glomerata algae and bleached eucalyptus pulp. Cellul. 23 (1), 493–503.

Yang, Q., Zhao, D., Liu, Q., 2020. Connections between amino acid metabolisms in plants: lysine as an example. Front. Plant Sci. 11, 928.

Zanchetta, E., Damergi, E., Patel, B., Borgmeyer, T., Pick, H., Pulgarin, A., Ludwig, C., 2021. Algal cellulose, production and potential use in plastics: Challenges and opportunities. Algal Res. 56, 102288.

Zhu, Z., Sathitsuksanoh, N., Zhang, Y.-H.-P., 2009. Direct quantitative determination of adsorbed cellulase on lignocellulosic biomass with its application to study cellulase desorption for potential recycling. Analyst 134 (11), 2267–2272.

Zrimec, M.B., Malta, E., Dunbar, M.B., Cerar, A., Reinhardt, R., Mihelič, R., 2022. Wastewater Cultivated Macroalgae as a Bio-resource in Agriculture. Sustainable Global Resources of Seaweeds 1, 435–449.